CALIBRATION OF BONDING MODEL PARAMETERS FOR COATED FERTILIZERS BASED ON PSO-BP NEURAL NETWORK

/

基于 PSO-BP 神经网络的包膜肥料 Bonding 模型参数标定

Xin Du, Cailing Liu*), Meng Jiang, Hao Yuan, Lei Dai, Fanglin Li, Zhanpeng Gao
College of Engineering, China Agricultural University, Beijing 100083/ China;
Tel: 0086-010-62737502; E-mail: cailingliu@163.com
Corresponding author: Cailing Liu
DOI: https://doi.org/10.35633/inmateh-65-27

Keywords: *Coated fertilizer; Parameter calibration; Proxy Model; PSO-BP Neural Network*

ABSTRACT

In this paper, the ultimate crushing displacement Y_1 and load Y_2 of the coated fertilizer granules were obtained by uniaxial compression test as 0.450 mm and 58.668 N, respectively. The Plackett-Burman and Steepest ascent tests were taken to determine factors that had significant effects on the results and their ranges of values, respectively. Finally, the Particle Swarm Optimization - Back Propagation (PSO-BP) neural network was trained, and the correlation coefficients of training, validation, testing and overall performance were obtained as 0.98057, 0.95781, 0.96724 and 0.97459, respectively. The Y_1 and Y_2 are 0.450 mm and 58.703N, with a relative error of 0.06% from the actual value.

摘要

采用 PSO-BP 神经网络模型为代理模型对 Bonding 模型参数进行标定，首先通过单轴压缩试验得到包膜肥料颗粒的极限破碎位移和极限破碎载荷分别为 0.450 mm 和 58.668 N。建立包膜肥料的 DEM 模型，分别采取 Plackett-Burman 和 Steepest ascent test 确定对结果影响显著的因素及其取值范围。采用全因素试验数据训练 PSO-BP 神经网络，得到训练过程、验证过程、测试过程和整体性能的相关系数分别 0.98057、0.95781、0.96724 和 0.97459，表明训练后的 PSO-BP 神经网络拟合效果良好，可以预测极限破碎位移和极限破碎载荷。PSO-BP 神经网络预测结果显示，当法向刚度 X_1、切向刚度 X_2、切向极限应力 X_4 和粘结半径 X_5 分别为 1.006E+10 N/m²、1.021E+10 N/m²、1200000Pa 和 0.20 mm 时，压缩位移 Y_1 和压缩载荷 Y_2 分别为 0.450 mm 和 58.703 N，与实际值相对误差最小为 0.06%。

INTRODUCTION

Fertilizers play a significant role in increasing crop yields, and China uses a large amount of chemical fertilizers with low fertilizer utilization rates *(Chojnacka et al., 2020)*. Controlled release fertilizer adopts polymer coating, which can quantitatively control the amount and period of fertilizer nutrient release, so that the effect of fertilizer saving and efficiency is significant *(Xiang et al., 2017)*. The nutrient release characteristics of wrapper fertilizers are closely related to the material and structure of the wrapper layer *(Chen et al., 2018)*, mechanical damage can cause damage to the envelope layer and thus affect the nutrient release characteristics of the fertilizer. In order to study the principle of mechanical damage of wrapped fertilizer, the discrete element method is proposed to be used for numerical simulation of the crushing process.

The calibration process of numerical simulation parameters directly affects the accuracy of simulation results *(Coetzee, 2017)*. Researchers have tried many methods to calibrate or measure discrete component parameters. One is to measure the parameters of the particle directly by experiment, which is applicable to the parameters that reflect the nature of the particle itself such as Poisson's ratio, density, shear modulus, etc.; the other is to measure the macroscopic phenomenon of the particle by experiment and then reversely calibrate it. In the inverse calibration process, the traditional method is "trial and error", which is inefficient and inaccurate *(Chen, 2017)*. To remedy these deficiencies, Zhao *(Zhao et al., 2012)* attempted to explore the complex relationships between micro- and macro-mechanical behaviors and parameters through empirical or theoretical formulations.

Xin Du, Ph.D. Stud.; Cailing Liu, Prof. Ph.D.; Meng Jiang, Ph.D. Stud.; Hao Yuan, Ph.D. Stud.; Lei Dai, Ph.D. Stud.; Fanglin Li, Ph.D. Stud.; Zhanpeng Gao Ph.D. Stud.*

During the calibration process, samples were generated using design of experiments methods, such as Yoon *(Yoon, 2007)* using central combined design (CCD), Hanley *(Hanley et al., 2011)* using Taguchi method and orthogonal tests, Rackl *(Rackl and Hanley, 2017)* using Latin hypercube sampling and Kriging methods. Optimization algorithms were then used to process the data and obtain calibration results, such as Do *(Do et al., 2018)* using genetic algorithms, Benvenuti *(Benvenuti et al., 2016)* using artificial neural networks, and Zhou *(Zhou et al., 2018)* using radial basis neural network method. However, the above studies still have some shortcomings. On the one hand, the above calibration methods simplify the parameters, and there are few studies on multi-parameter multi-objectives. On the other hand, the accuracy of the obtained models is low, and it is difficult to predict the combination of simulation parameters accurately.

In this paper, the ultimate crushing load and loading displacement of wrapped fertilizer particles were measured by uniaxial compression test, and by establishing the same simulation model as the real test, the number of factors was gradually reduced and the range of factor values was narrowed by using PB design and the most rapid ascent method, and then the PSO-BP neural network was trained by using the full-factor test to predict the Bonding model parameter combinations with the well-fitted network model, and the obtained parameter combinations were validated. The Bonding model parameters of the envelope fertilizer were accurately calibrated.

MATERIALS AND METHODS

Bonding Model

In the Bonding model, the material being crushed (particles, blocks, etc.) it consists of a number of small particles, which are held together by bonded cements. Bonded cements have mechanical properties similar to those of the finite element method and are subject to deformation (tension, compression, torsion) under external forces. When the force or moment generated by the deformation of bonded cements reaches a certain level, the cements break and the small particles separate from each other. The Bonding model assumes that the cement between two particles is a virtual flat plate (cylinder), as shown in Figure 1. When the relative motion of two particles occurs, the flat plate (cylinder) is subjected to tension, bending and shear, and the mile generated by the bond can be obtained according to the following equation.

$$\begin{cases} \delta F_n = -v_n S_n A \delta t \\ \delta F_t = -v_t S_t A \delta t \\ \delta M_n = -\omega_n S_t J \delta t \\ \delta M_t = -\omega_t S_n \dfrac{J}{2} \delta t \end{cases} \tag{1}$$

where: δF_n and δF_t are the normal and tangential forces respectively; v_n and v_t are the normal and tangential velocities of the particles respectively; S_n and S_t are the normal stiffness and tangential stiffness respectively; δt is the simulation time step; A is the contact area between the particles of "fraction"; δM_n and δM_t are respectively tangential moment and normal moment; ω_n, ω_t are the normal and tangential angular velocities, respectively; J is the polar moment of inertia of the cement.

$$\begin{cases} A = \pi R_B^2 \\ J = \dfrac{1}{2} \pi R_B^4 \end{cases} \tag{2}$$

where: R_B is the bonded radius of the cement. It can be seen from formulas (1) and (2) that the bonded radius R_B has a direct effect on the force and moment.

When the force and moment reached the limit value or the distance between the "fraction" particles is greater than the setting contact radius, the bonded cement will break. The normal and tangential shear force calculation formulas are as follows:

$$\begin{cases} \sigma_{\max} < \dfrac{-F_n}{A} + \dfrac{2M_t}{J} R_B \\ \tau_{\max} < \dfrac{-F_t}{A} + \dfrac{M_n}{J} R_B \end{cases} \tag{3}$$

where: σ_{max} is the normal shear force; τ_{max} is the tangential shear force.

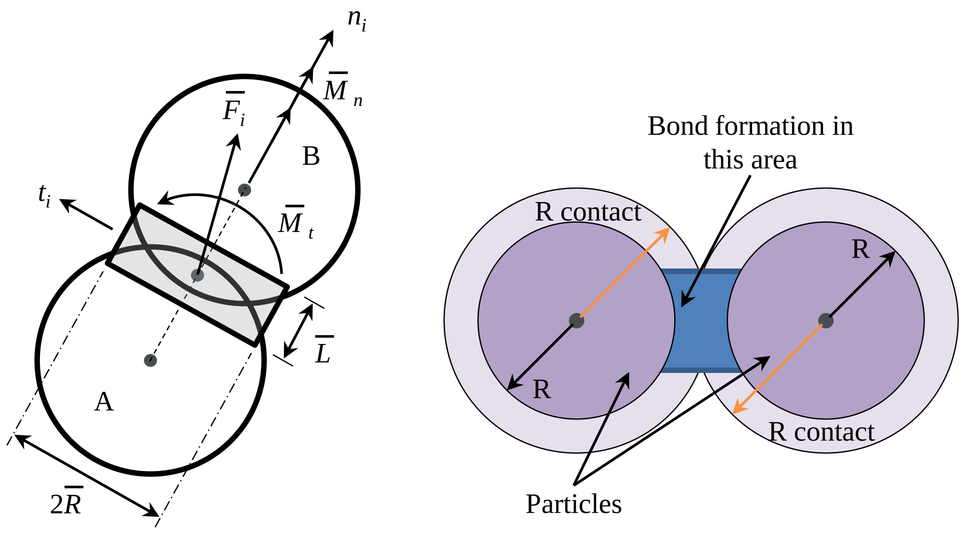

(a) Bonding model schematic (b) Schematic diagram of particles bonding

Fig. 1 – Bonding model schematic

F_i is the contact force vector, which can be resolved into normal and shear components; M_n and M_t denote the axial- and shear- directed moments, respectively; n_i and t_i are the unit vectors that define the contact plane; L and R_i are the length and parallel-bond radius of the cement; A and B denote two particles in contact; R and R contact denote the radius and contact radius between two particles, respectively.

Material parameters

In this paper, the coated controlled-release fertilizers were sourced from Shandong Nongyang Biological Technology Co., Ltd., China. The moisture content, true density, average triaxial size, equivalent diameter and sphericity of fertilizer are 0.88%, 1.46 g/cm^3, 4.08 mm×3.97 mm×3.89 mm, 3.98 mm and 0.975, respectively. Select fertilizers (as shown in Fig. 2(a) (b)) whose length, width and height are similar to the equivalent diameter to establish a contour model. To study the fertilizer particle fragmentation characteristics, the bonded particle method (BMP) was used to build a discrete element model of fertilizer particles (as shown in Fig. 2(c)).

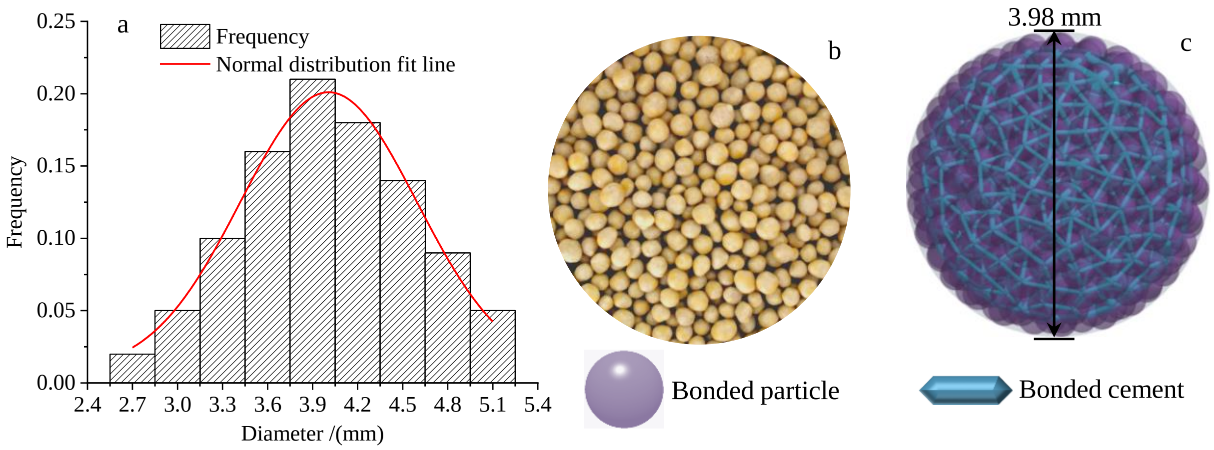

Fig. 2 – Fertilizers and discrete element model

Uniaxial compression test (actual)

Select fertilizer particles with a diameter of 3.98 mm, and use a universal tester to perform a uniaxial compression test on the fertilizer particles, and load them at a speed of 0.05 mm/s until the sample is damaged, as shown in Fig. 3(a). The experiment was repeated 20 times and the average value was taken, then the displacement load curve of the fertilizer particles was obtained as shown in Fig. 3(b).

As can be seen from Fig. 3, the ultimate crushing displacement and ultimate crushing load of the coated fertilizer granules were obtained by uniaxial compression test as 0.450 mm and 58.668 N, respectively.

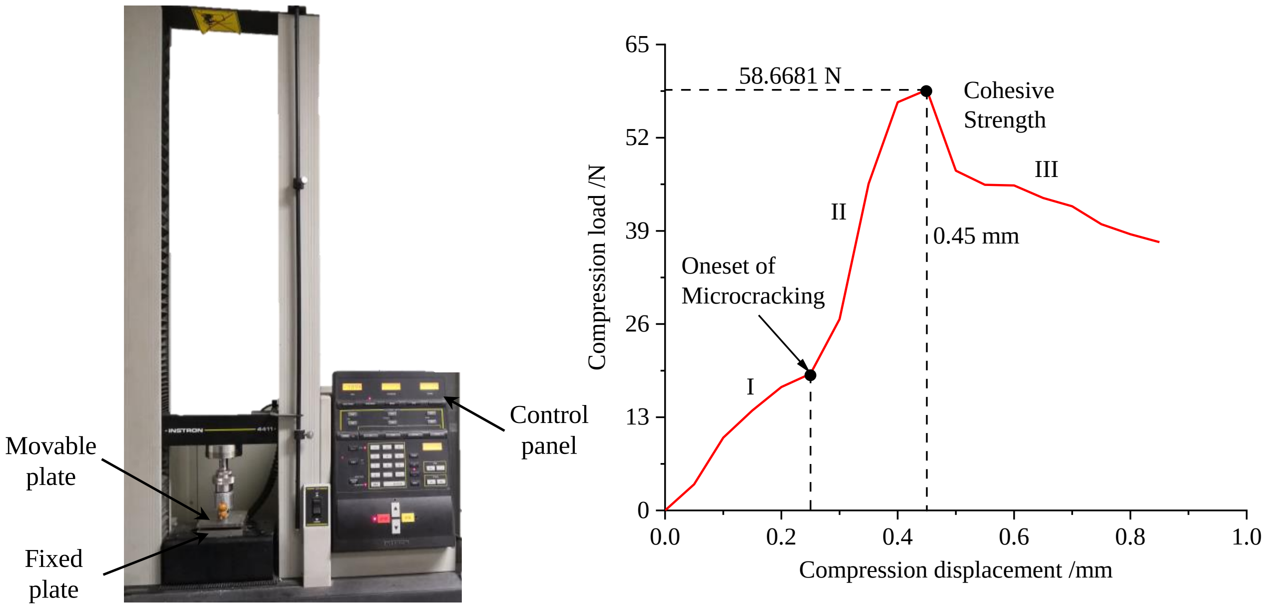

(a) Universal testing machine (b) Displacement-load curve

Fig. 3 – Uniaxial compression test

Uniaxial compression test (simulation)

The discrete element software EDEM2018 was used to establish a uniaxial compression simulation test consistent with the actual test, as shown in Fig. 4. The constitutive and contact parameters of the coated fertilizer particles used in the simulation refer to related literature *(Du Xin et al., 2019; Liu Cailing et al., 2018)*, and the values are shown in Table 1.

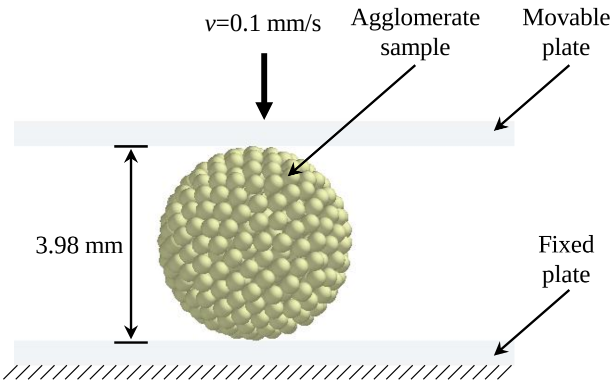

Fig. 4 – Simulation diagram of uniaxial compression test

Table1

Simulation parameters

Parameter	Fertilizer	ABS
Poisson's ratio	0.225	0.394
Real density (kg/m^3)	2474	1060
Shear modulus (Pa)	1.528×10^8	8.9×10^8
Collision recovery factor	0.654	0.47
Coefficient of static friction	0.189	0.42
Rolling friction coefficient	0.034	0.095

PSO-BP neural network

The standard BP neural network (three-layer model) structure is used, i.e., input layer, implicit layer and output layer. The BP neural network uses the gradient correction method for learning the weights and thresholds. Suitable parameters can effectively improve the overall performance of the system. Two important factors that affect the learning quality of BP neural networks are: the number of implicit nodes and the size of learning rate. The increase in the number of implicit nodes accelerates the decrease in error, but the computational effort also increases and the learning time of the system becomes longer, which reduces the usefulness of the system. The number of implicit neurons is estimated using the following formula:

$$j = \sqrt{i+k} + z \tag{4}$$

where j is the number of neurons in the hidden layer, i is the number of neurons in the input layer, k is the number of neurons in the output layer, and z is the empirical value ($1 \le z \le 10$).

The learning rate determines the size of the change in weights and thresholds during each iteration. Decreasing the learning rate can reduce the probability of the system falling into local convergence and make the system eventually converge globally; too small a learning rate results in a small change in each iteration, leading to an increase in the number of iterations and a longer training and learning time.

Different combinations of the number of implied nodes and learning rate are used to form different network structures and compare the final error output of the system. Considering the learning time and the final error of the network, the best learning ability of the BP neural network is obtained when the number of implicit nodes of this system is 10 and the learning rate is 0.3.

The standard BP neural network can approximate any nonlinear continuous function, but the algorithm has the defects of slow convergence and easily falling into local minima. In order to find better network weights and threshold values for BP neural networks and minimize their global errors, the PSO algorithm is used to optimize the BP neural networks.

The PSO algorithm is an evolutionary search technique proposed based on birds' predatory behavior and movement patterns. Each bird is equivalent to a particle in the model, representing the solution of the optimization problem, and their range and direction depend on the velocity of each particle in the particle swarm, and the best adaptation value is obtained by the optimal particle searching in the solution space for the global optimal solution.

Assuming that there are M particles forming a particle population in a D-dimensional search space, the main computational derivation of the PSO algorithm is:

$$\begin{cases} v_{id}^{(t+1)} = u \times v_{id}^{(t)} + c_1 r_1 \left(P_{id} - x_{id}^{(t)}\right) + c_2 r_2 \left(P_{gd} - x_{id}^{(t)}\right) \\ x_{id}^{(i+1)} = x_{id}^{(t)} + x_{id}^{(t+1)} \end{cases} \tag{5}$$

where: $v_i = (v_{i1}, v_{i2}, \ldots, v_{id})$ denotes the velocity of the i-th particle; $x_i = (x_{i1}, x_{i2}, \ldots, x_{id})$, ($i = 1, 2, \ldots, M$) denotes the position of the particle in space; $P_i = (P_{i1}, P_{i2}, \ldots, P_{id})$ denotes the historical best position passed by the i-th particle in space; $P_g = (P_{g1}, P_{g2}, \ldots, P_{gd})$ denotes the historical best position passed by the whole population in space; c_1, c_2 denote the learning acceleration coefficients, which usually take the value of 2.0; r_1, r_2 are random numbers varying between [0,1]; u denotes the inertia weights.

The weights and thresholds of the BP neural network are regarded as particles, and the training process of the system is completed by mutual learning between particles, then the change of the weights is:

$$\Delta W_{ij} = c_1 r_1 \left(W_{ij}(p) - W_{ij}\right) + c_2 r_2 \left(W_{ij}(g) - W_{ij}\right) \tag{6}$$

where $W_{ij}(p)$ denotes the individual optimal value of the corresponding particle; $W_{ij}(g)$ denotes the global optimal value of the whole network.

The flow chart of BP neural network weights modified by PSO algorithm is shown in Fig. 5. The specific training process of the network is as follows.

(1) Initialize the PSO algorithm parameters. Determine the initial and ending weights according to the structural characteristics of the BP neural network, learn the acceleration coefficients and the initial positions of the particle population.

(2) The PSO algorithm corresponds to the BP neural network. A D-dimensional vector is created, which represents a particle in the PSO algorithm and includes the weights and thresholds of the implicit and output layers in the BP network.

(3) Calculate the fitness of the particles. In order to measure the goodness of the particle position, the fitness function needs to be established, using the error function in the BP network as the fitness function.

(4) Update individual optima and global optima. Compare the fitness function values of each particle at time t-1 with those at time t. If the fitness of the particle is better at time t, the individual optimum of the corresponding particle is updated. Similarly, compare the fitness function values of the population at time t-1 with those at time t. If the fitness of the population is better at time t, then the global optimum of the population is updated.

(5) Update the position and velocity of the particles. The velocity and position information of the particles are recalculated according to Eqs. (2) and (4), and the weights and thresholds of each layer are updated.

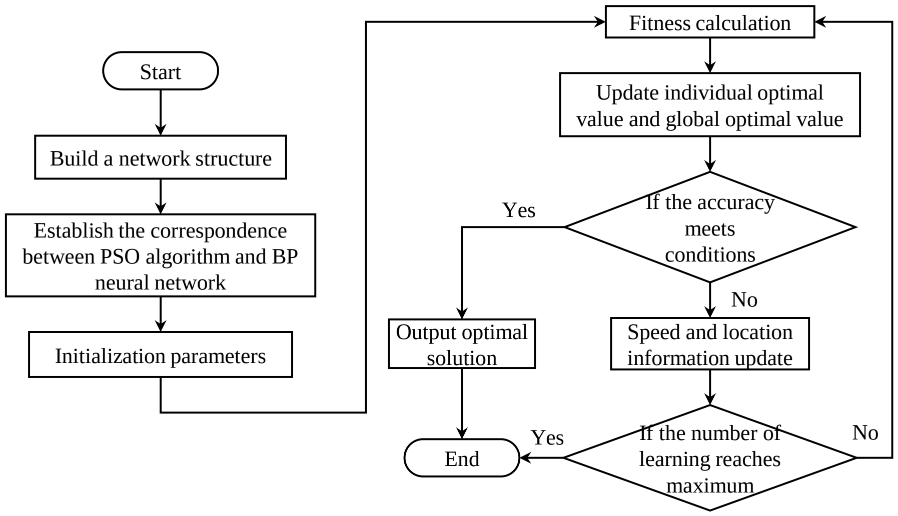

Fig. 5 – Fertilizer granule crushing test

RESULTS

Plackett-Burman test

The normal stiffness, tangential stiffness, normal ultimate stress, tangential ultimate stress and bonded radius were used as the five factors (X_1, X_2, X_3, X_4, X_5) of the Plackett-Burman test, and two levels of each factor were selected.

The Plackett-Burman design with N=11 was chosen for the test, and six dummy terms were reserved for error analysis, and the Plackett-Burman test protocol and results are shown in Table 2, and the ANOVA and t-test were performed separately for each factor effect using Design-Expert 8.0.6 software, and the results are shown in Table 3.

Table 2

Plackett-Burman test results

No.	X_1	X_2	X_3	X_4	X_5	Y_1	Y_2
1	9.60E+09	1.28E+10	6.00E+05	1.20E+06	0.16	0.395	37.274
2	9.60E+09	1.28E+10	4.00E+05	8.00E+05	0.24	0.521	85.528
3	6.40E+09	1.28E+10	4.00E+05	1.20E+06	0.16	0.355	31.243
4	9.60E+09	1.92E+10	6.00E+05	8.00E+05	0.16	0.348	39.621
5	9.60E+09	1.92E+10	4.00E+05	8.00E+05	0.16	0.348	39.621
6	6.40E+09	1.92E+10	6.00E+05	8.00E+05	0.24	0.428	75.203
7	6.40E+09	1.92E+10	6.00E+05	1.20E+06	0.16	0.363	40.406
8	9.60E+09	1.28E+10	6.00E+05	1.20E+06	0.24	0.530	97.275
9	6.40E+09	1.92E+10	4.00E+05	1.20E+06	0.24	0.475	91.781
10	6.40E+09	1.28E+10	4.00E+05	8.00E+05	0.16	0.357	31.481
11	6.40E+09	1.28E+10	6.00E+05	8.00E+05	0.24	0.484	79.520
12	9.60E+09	1.92E+10	4.00E+05	1.20E+06	0.24	0.488	94.295

Table 3

Analysis of significance of parameters in Plackett-Burman test

	Compression Displacement					Compression Load				
Source	Sum of Squares	df	Mean Square	*F* Value	*p*-value	Sum of Squares	df	Mean Square	*F* Value	*p*-value
Model	0.055	5	0.011	42.07	0.0001*	8046.936	5	1609.387	73.06	< 0.0001*
X_1	0.002	1	0.002	9.02	0.0239*	159.034	1	159.034	7.22	0.0362*
X_2	0.003	1	0.003	11.81	0.0139*	27.941	1	27.941	1.27	0.3031
X_3	0.000	1	0.000	0.01	0.9439	1.581	1	1.581	0.07	0.7978
X_4	0.001	1	0.001	4.62	0.0753	144.188	1	144.188	6.55	0.0430*
X_5	0.048	1	0.048	184.92	< 0.0001*	7714.192	1	7714.192	350.17	< 0.0000*
Residual	0.002	6	0.000			132.178	6	22.030		
Cor Total	0.056	11				8179.114	11			

Notes：*Shows that the term is significant (i.e., $P < 0.05$).

Steepest ascent test

According to the Plackett-Burman test results, the initial values of the selected factors X_1, X_2, X_4 and X_5 were 8.00×10^9 N/m^2, 1.60×10^{10} N/m^2, 1.00×10^6 Pa and 0.18 mm, and the step length was 0.80×10^9 N/m^2, -0.16×10^{10} N/m^2, 0.10×10^{10} Pa and 0.01 mm, respectively. Based on the above description, a steepest ascent test was carried out to further find the parameters combination that approximates the true value. The steepest ascent test plan and results were shown in Table 4.

Table 4

Steepest ascent test plan and results

No.	X_1	X_2	X_4	X_5	Y_1	Y_2
1	8.00E+09	1.60E+10	1.00E+06	0.18	0.409	52.517
2	8.80E+09	1.44 E+10	1.10E+06	0.19	0.420	57.086
3	9.60E+09	1.28E+10	1.20E+06	0.20	0.446	63.534
4	1.04E+10	1.12E+10	1.30E+06	0.21	0.498	75.726
5	1.12E+10	9.60E+09	1.40E+06	0.22	0.510	78.411

From the test results in Table 5, it can be seen that the error between the compressive displacement and load in the simulation test and the real value first decreases and then increases, combined with 2.3.1, it can be seen that the actual uniaxial compressive displacement and load of fertilizer granules are 0.45 mm and 58.668 N respectively, and the compressive displacement Y_1 and load Y_2 of the 3rd group test are closest to the real value.

PSO-BP neural network

As can be seen from Table 5, the actual loading displacement and ultimate load are between the results of Scheme 1 and Scheme 4, therefore, the factor ranges of Scheme 1 and Scheme 4 were selected to complete the full-factor test with 4 factors and 4 levels, and the test factor level ranges are shown in Table 5.

Table 5

Table of test factor levels

Factor	Level			
	1	2	3	4
X_1	8.00E+09	8.80E+09	9.60E+09	1.04E+10
X_2	1.60E+10	1.44 E+10	1.28E+10	1.12E+10
X_4	1.00E+06	1.10E+06	1.20E+06	1.30E+06
X_5	0.18	0.19	0.2	0.21

The objectives to be optimized in this paper are compression displacement Y_1 and compression load Y_2. According to the importance of each objective, the linear weighted combination method is used to transform the multi-objective optimization problem into a single-objective optimization problem, and the index conversion and weighting formulas are as follows.

$$\begin{cases} \min \sum_{i=1}^{2} w_i y_i\left(x\right) \\ y_i = \left|\dfrac{Y_{ij}-Y_{io}}{Y_{io}}\right| \times 100\% \quad j \in \left[1, 256\right] \end{cases} \tag{7}$$

where:

w_i is the weighting factor, $w_1 = w_2$=0.5 in this paper; y_i is the relative error of each index and the actual value; Y_{ij} is the simulation result of each index of each scheme; Y_{io} is the actual value of each index, where Y_{1o}=0.45 mm, Y_{2o}=58.668 N.

There are 256 sets of simulation results, 180 sets are randomly selected as training network, and the other data are used as validation and testing network performance, and the correlation coefficients of training process, validation process, testing and overall performance of PSO-BP neural network are obtained as 0.98057, 0.95781, 0.96724 and 0.97459, respectively (as shown in Fig. 6). In general, a correlation coefficient greater than 0.9 is considered a good network fit *(Dong et al., 2020)*.

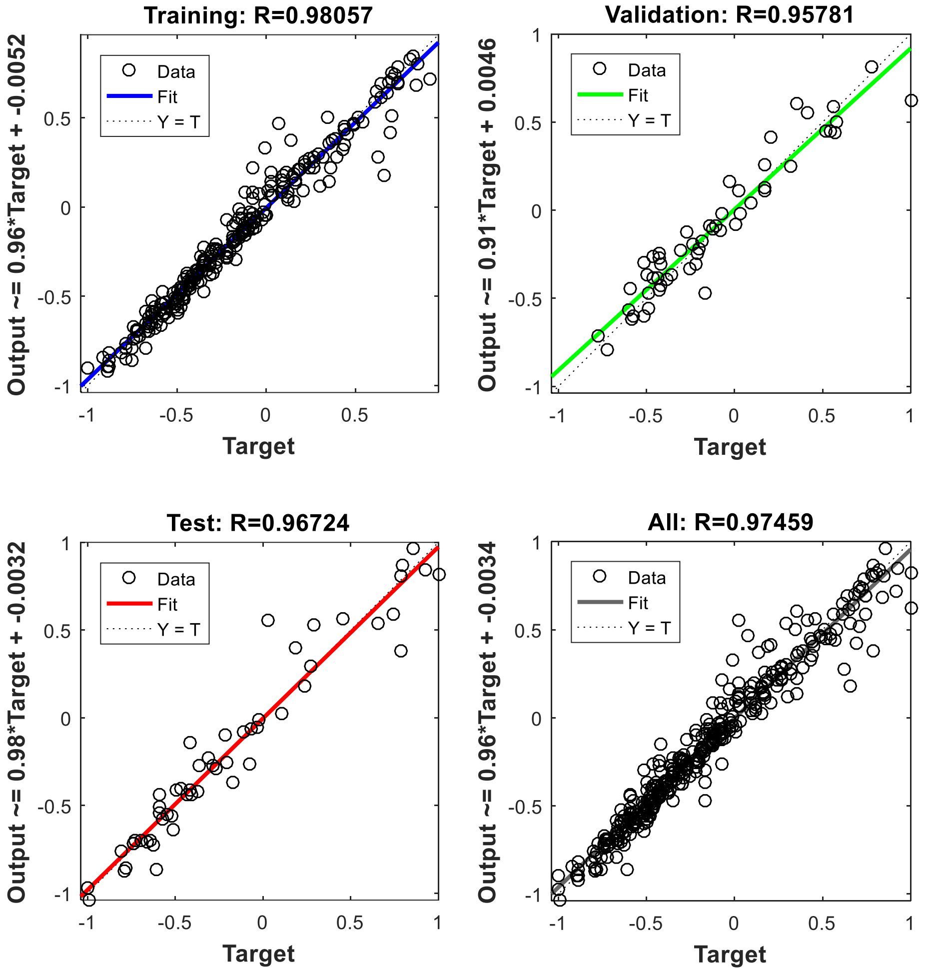

Fig. 6 – Simulation diagram of fertilizer particle crushing during fertilizer discharge process

Combined with the relative error between the validation set, test set and the real value from Fig. 7, it can be concluded that the PSO-BP neural network fitted in this paper can realistically predict the fertilizer granule crushing.

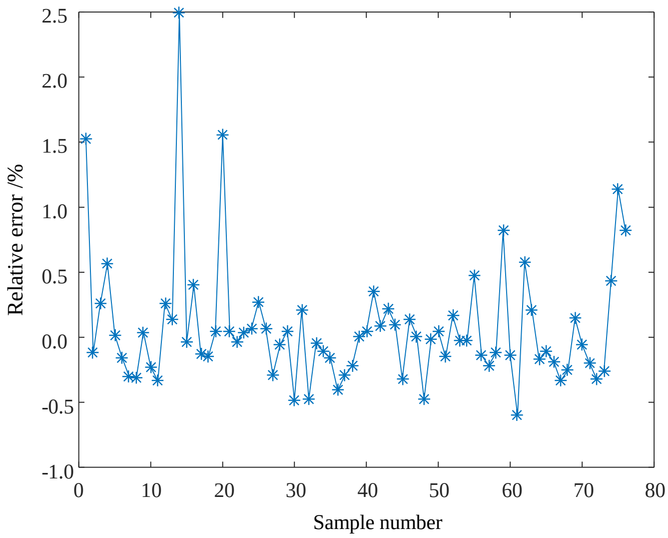

Fig. 7 – Relative error of validation set, test set and true value

With the above trained PSO-BP neural network model as the objective function, the compression displacement Y_1 and compression load Y_2 are optimized, and the network input that makes the network output 0 (with zero relative error to the true value) is solved to obtain a series of parameter combinations, which are inverted and substituted into EDEM to verify the rationality of the parameter combinations (as shown in Table 6).

Table 6

Parameter combination verification results

No.	X_1	X_2	X_4	X_5	Y_1	Y_2	y_1	y_2	y
1	9.979E+09	1.036E+10	1200000	0.20	0.455	59.524	1.111	1.459	2.570
2	1.006E+10	1.021E+10	1200000	0.20	0.450	58.703	0.000	0.060	0.060
3	1.008E+10	1.019E+10	1200000	0.20	0.451	58.594	0.222	0.126	0.348
4	9.948E+09	1.031E+10	1200000	0.20	0.452	58.941	0.444	0.466	0.910
5	1.003E+10	1.038E+10	1200000	0.20	0.452	59.395	0.444	1.238	1.683

The simulation results of the five parameter combinations in Table 7 show that the relative error y is 0.06%~2.57%, which indirectly proves that the PSO-BP neural network model fits well. When the normal stiffness X_1, tangential stiffness X_2, tangential ultimate stress X_4 and bonded radius X_5 are 1.006E+10 N/m^2, 1.021E+10 N/m^2, 1200000 Pa and 0.20 mm, respectively, the compression displacement Y_1 and compression load Y_2 are 0.450 mm and 58.703 N, respectively, with the minimum relative error of 0.06%.

CONCLUSIONS

The ultimate crushing displacement and ultimate crushing load of the encapsulated fertilizer granules were obtained by uniaxial compression tests as 0.450 mm and 58.668 N, respectively. The PSO-BP neural network model was used as a proxy model to calibrate the Bonding model parameters, and the factors with significant effects on the results and their value ranges were determined by the Plackett-Burman and Steepest ascent tests, respectively. The full-factor test data were used to train the PSO-BP neural network, and correlation coefficients of 0.98057, 0.95781, 0.96724 and 0.97459 were obtained for the training process, validation process, testing process and overall performance, respectively. The prediction results of PSO-BP neural network show that when the normal stiffness X_1, tangential stiffness X_2, tangential ultimate stress X_4 and bonded radius X_5 are 1.006E+10 N/m^2, 1.021E+10 N/m^2, 1200000 Pa and 0.20 mm, respectively, the compression displacement Y_1 and compression load Y_2 are 0.450 mm and 58.703 N, with a minimum relative error of 0.06% from the actual value.

ACKNOWLEDGEMENT

This work was financially supported by National Key Research and Development Plan of China (2017YFD0700703).

REFERENCES

[1] Benvenuti, L., Kloss, C., Pirker, S., (2016). Identification of DEM simulation parameters by Artificial Neural Networks and bulk experiments. *Powder Technology*, 291:456-465.

[2] Chen, P.Y., (2017). Effects of Microparameters on Macroparameters of Flat-Jointed Bonded-Particle Materials and Suggestions on Trial-and-Error Method. *Geotechnical and Geological Engineering*, 35 (2):663-677.

[3] Chen, S., Yang, M., Ba, C., et al, (2018). Preparation and characterization of slow-release fertilizer encapsulated by biochar-based waterborne copolymers. *Science of the Total Environment*, 615:431-437.

[4] Chojnacka, K., Moustakas, K., Witek-Krowiak, A., (2020). Bio-based fertilizers: A practical approach towards circular economy. *Bioresource Technology*, 295:122223.

[5] Coetzee, C.J., (2017). Review: Calibration of the discrete element method. *Powder Technology*, 310:104-142.

[6] Do, H.Q., Aragón, A.M., Schott, D.L., (2018). A calibration framework for discrete element model parameters using genetic algorithms. *Advanced Powder Technology*, 29 (6):1393-1403.

[7] Dong, Y., Fu, Z., Peng, Y., et al, (2020). Precision fertilization method of field crops based on the Wavelet-BP neural network in China. *Journal of Cleaner Production*, 246:118735.

[8] Du, X., Liu, C., Jiang, M., et al, (2019). Design and experiment of self-disturbance inner-filling cell wheel maize precision seed-metering device. (自扰动内充型孔轮式玉米精量排种器设计与试验) *Transactions of the Chinese Society of Agricultural Engineering*, 35 (13):23-34.

[9] Hanley, K.J., O'Sullivan, C., Oliveira, J.C., et al, (2011). Application of Taguchi methods to DEM calibration of bonded agglomerates. *Powder Technology*, 210 (3):230-240.

[10] Liu, C., Wei, D., Song, J., et al, (2018). Systematic Study on Boundary Parameters of Discrete Element Simulation of Granular Fertilizer. (颗粒肥料离散元仿真边界参数系统化研究) *Transactions of the Chinese Society for Agricultural Machinery*, 49 (09):82-89.

[11] Rackl, M., Hanley, K.J., (2017). A methodical calibration procedure for discrete element models. *Powder Technology*, 307:73-83.

[12] Xiang, Y., Ru, X., Shi, J., et al, (2017). Preparation and properties of a novel semi-IPNs slow-release fertilizer with the function of water retention. *Journal of Agricultural and Food Chemistry*.

[13] Yoon, J., (2007). Application of experimental design and optimization to PFC model calibration in uniaxial compression simulation. *International Journal of Rock Mechanics and Mining Sciences*, 44 (6):871-889.

[14] Zhao, G., Dai, B., Ma, C., (2012). Study of effects of microparameters on macroproperties for parallel bonded model. *Yanshilixue Yu Gongcheng Xuebao/Chinese Journal of Rock Mechanics and Engineering*, 31 (7):1491-1498.

[15] Zhou, H., Hu, Z., Chen, J., et al, (2018). Calibration of DEM models for irregular particles based on experimental design method and bulk experiments. *Powder Technology*, 332:210-22